J Mater Sci: Mater Med (2010) 21:1811–1816
DOI 10.1007/s10856-010-4052-2

The mechanical anisotropy on a longitudinal section of human enamel studied by nanoindentation

Zhen-jiang Cheng · Xiu-mei Wang · Jun Ge · Jian-xin Yan · Ning Ji · Li–li Tian · Fu-zhai Cui

Received: 23 February 2009 / Accepted: 2 March 2010 / Published online: 13 March 2010

Abstract Nanoindentation has been widely used for probing the mechanical properties of tooth, especially for characterizing its complex hierarchical structures. Previous studies have confirmed the anisotropic mechanical behaviors caused by the alternated orientations of enamel rods and the alignment of fibril-like hydroxyapatite crystals, but the longitudinal section of enamel, which was composed of parallel-arranged rods, was regarded as a homogeneous continuum as always. In this study, nanoindentation combined with SEM was carried out with the indenter rotating on the longitudinal section of enamel to evaluate the relativity between the nano-mechanical properties and the orientation of indentation impressions. It has been shown that the enamel presented different elastic modulus and hardness with different angles of indenter on its longitudinal section, and its anisotropy was also confirmed by the remarkable asymmetric morphologies of impressions. We observed that the parallel arrangement of crystal fibrils and enamel rods might trigger the expansion of the microcracks in preferred orientation, and result in scalene triangle indentation impressions, altering contact areas as well as inconsistent mechanical behaviors. Consequently, it is considered that the longitudinal sections of enamel should be modeled as anisotropic.

Z. Cheng · X. Wang · J. Ge · F. Cui (✉)
Laboratory of Advanced Materials, State Key Laboratory of New Ceramic and Fine Processing, Department of Materials Science and Engineering, Tsinghua University, YiFu Technology and Science Building, Room 2336, Beijing 100084, People's Republic of China
e-mail: cuifz@mail.tsinghua.edu.cn

J. Yan · N. Ji
The China Crest Research Institute of P&G, Beijing 100084, People's Republic of China

L. Tian
Department of Stomatology, China-Japan Friendship Hospital, Beijing 100029, People's Republic of China

1 Introduction

Dental enamel is a type of mineralized material with highly complex hierarchical structure, which is mainly composed of aligned rods of 6–8 μm in diameter arranged nearly perpendicular to the tooth surface [1]. Each rod consists primarily of fibril-like hydroxyapatite crystals (nearly 30 nm in diameter). These HAP crystals tend to align lengthways and lie parallel to the rod axis along the center, in spite of the existence of incoherence of combining crystals of different orientations at the rod boundary. Due to the complex hierarchical structural organization and distinct composition of enamel, the mechanical properties in differenct districts differ significantly [2–4].

Investigation of the mechanical properties of tooth enamel is of particular challenge in virtue of its complex hierarchical structures. Nanoindentation is now widely used for probing the mechanical properties of small volumes, thin films, small micro-structural features and also biological hard tissues. Nanoindentation has already been proved to be an excellent technique to study the mechanical behavior of tooth, especially for characterizing its complex hierarchical structure. Previous studies have shown that nanoindentation examinations revealed the hardness and elastic modulus decreased on traversing from the occlusal surface to DEJ (dentine-enamel junction); differed from the lingual to buccal sides of the molar; increased from the tail area to the center in a single enamel rod [4–9]. In these studies, the longitudinal section of enamel was modeled as a homogeneous and isotropic continuum, and little attention had been paid on the influence of the angle between the nano-indenter and enamel rods' orientations. These results are similar to the experiments conducted by Nanako Iwamoto, in which different anisotropies of dentin with respect to its fracture toughness were identified, when placed on the plane of crack propagation parallel and aligned or transverse to the plane of dentinal tubules [10]. Whether the mechanical behaviors of the longitudinal section of enamel were affected by the different orientations of indenters relative to the alignment of crystals and enamel rods still remained unclear, especially for the nanoindentation tests on nano-scale, as the anisotropy maybe much more sensitive than micro-indentation.

The purpose of the present study was to investigate whether the rotation of the indenters exert certain effects on the examination of the nano-mechanical properties of enamel on a longitudinal section.

2 Materials and methods

2.1 Sample preparation

Mature human mandible incisors were all extracted from individuals as part of their dental treatment in The China Crest Research Institute of P&G in Beijing. The subscribers were aged from 15 to 30 years old, with no injured areas in their tooth. The incisors were saved in thymol solution 4°C after being sterilized with gamma ray. Before the following processes, the incisors were washed in the double distilled water, and air-dried. The enamel specimens for nanoindentation tests were prepared by hard tissue microtome (DELUXE 1000 SERIES HARD TISSUE MICROTOME-Scientific Fabrications 604 W. Kinmbark). The incisors were cut vertically so that the enamel rods were nearly parallel to the cut surface, as shown schematically in Fig. 1a–c. The enamel specimens were then embedded in polymethylmethacrylate at room temperature. The embedded samples were further polished through progressive grades of waterproof silicon carbide abrasive papers (320, 600, 1200, 2500 grit) under de-ionized water and polished on micro-cloths with successively finer grades of alumina powder by Phoenix 4000 Sample Preparation System (Buehler Ltd., Illinois, USA). Finally, the specimens were ultrasonically cleaned for 10 s to remove surface debris.

2.2 Nanoindentation

A Nanoindenter XP (MTS Systems Co., Oak Ridge, TN) was used to assess mechanical properties of the testing area

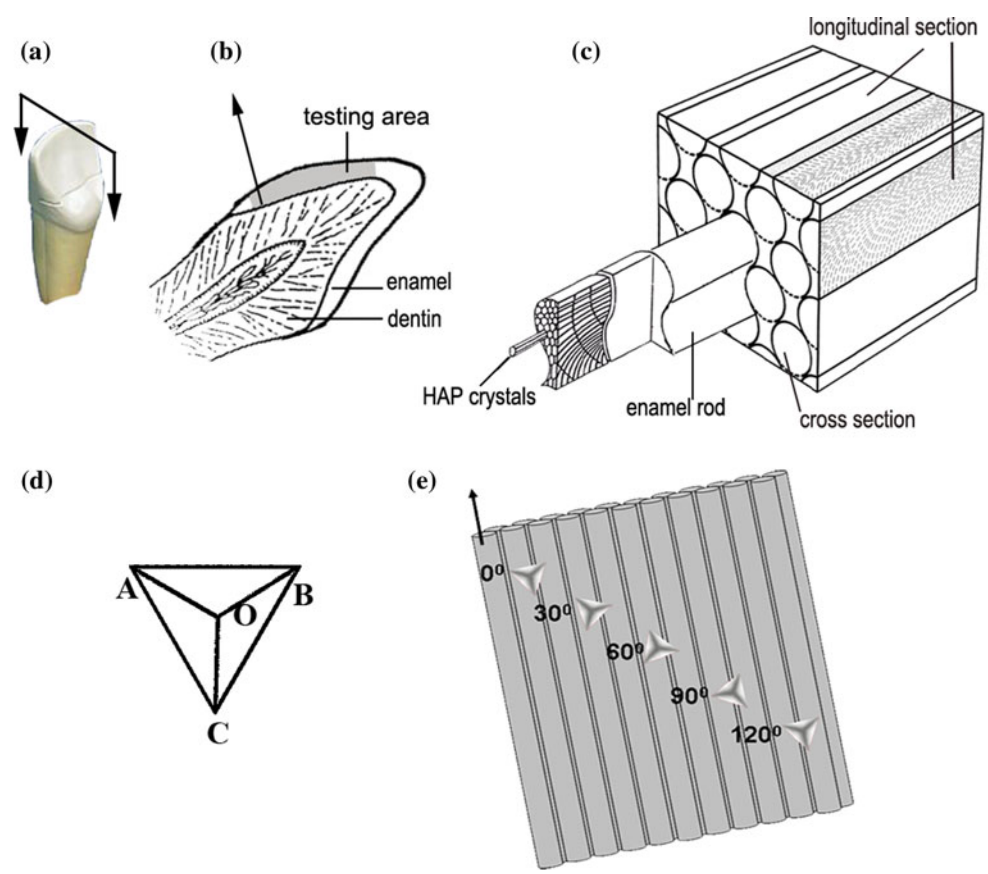

Fig. 1 Sketch of the preparation of the samples and nanoindentation test processes. **a** The *arrows* shows the cut directions. **b** The *arrows* in the testing area indicates the orientation of enamel rods. **c** Schematic illustration of the hierarchical assembly of enamel structure. **d** Shows the edges of a standard nanoindent impression. **e** Schematic diagram of the longitudinal section of outer enamel indicates the impressions with different angles from 0° to 120°. The arrow points to the orientation of enamel rods

shown in Fig. 1b at room temperature. The system had force and displacement resolution of 50 nN and 0.01 nm, respectively. The indentation depth and rate were 1000 nm and 10 nm/s. The Poisson's ratio and elastic modulus of the diamond Berkovich tip are 0.07 and 1140 GPa. As shown in Fig. 1d, the nanoindent impression has three edges (OA, OB, and OC). Fused silica, which exhibits elastic isotropy and has a relatively low modulus/hardness ratio, was used to calibrate the tip shape function. A fused silica sample was used as a standard calibration material to check on the quality of the measurements providing assurance that the machine was properly calibrated and the analysis procedures were properly implemented. Series of indentations were made in the resin domain of the samples to check whether the indentation impressions were regular triangular pyramid, to make sure that it was flat enough for following processes. In this experiment, nine groups of indentations were made in the testing area where the rods were parallel to each other and perpendicular to the DEJ. In this study, the angles between the orientations of OC and the longitudinal axis direction of enamel rods in nine groups were 0°, 15°, 30°, 45°, 60°, 75°, 90°, 105° and 120°, respectively, as schematically presented in Fig. 1e. Moreover, the two adjacent indentations should be placed more than 20 μm away from each other to avoid their interactions. Finally, nine groups of data were collected from the 27 nanoindentations in each sample. A total of six samples were tested, the data were analyzed using standard routines to calculate nanohardness and elastic modulus following Oliver–Pharr's method [11].

2.3 SEM observation

The specimens were sputter-coated with gold for 3 min and observed by scanning electron microscopy at 10 kV (LEO-1530, Germany).

3 Results

3.1 The relativity between the nano-mechanical properties of enamel and the orientation of indentation compressions

Nine groups of nanoindentation tests were conducted on the longitudinal sections of enamel with different rotations of the indenter. The values of the hardness and elastic modulus on the longitudinal sections exhibited significant difference, as shown in Fig. 2, which indicated the structural anisotropy of enamel. For example, the elastic modulus and hardness in the direction of 45° were 83.36 ± 1.71 and 3.83 ± 0.09 GPa, while they decreased to 74.78 ± 3.10, 3.26 ± 0.34 GPa, respectively in the direction of 0°.

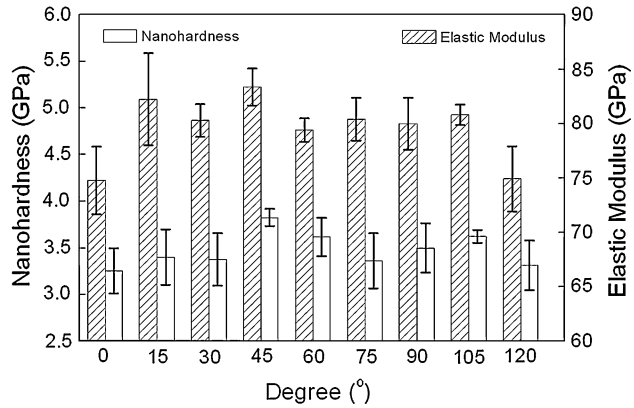

Fig. 2 The nanohardness and modulus after uploading are altered as the indenter rotates

3.2 The indentations presented as scalene tetrahedrons

In our nanoindentation examination, the distances between any two adjacent indent positions were arranged no less than 50 μm to avoid their interference. It has been shown that the mechanical properties of enamel rods altered with the rotation of the indenter, which could be visually reflected by the SEM topographies of the residual indent impressions (Fig. 3b–j). Unlike the typical triangular pyramid impressions in the resin region, the shapes of the residual indent impressions in the enamel region changed evidently with different lengths of pyramidal tetrahedron edges (OA, OB, and OC in Fig. 3). The lengths of OA, OB, and OC from each nanoindentation were calculated, and all the data from the same group were used for preliminary statistical analysis, respectively. The statistical values of OA, OB, and OC with respect to certain rotation angle of indenter were depicted in Fig. 4. Primitively, the edge of the indentation, OC, which was parallel to the rods, was evidently longer than OB and OA. As it was rotated by 15°, OC and OB became shorter appreciably, while OA extended dramatically. OA reached its longest value at 60° while OB reached its shortest at 30°, respectively. Also, the edge lengths varied cyclically when the angle was over (0°, 120°). It is noteworthy that the bright accumulation existed in the extended orientation of the longest edge (Fig. 3), which was caused by the expansion of the mineral when being pressured, as the stress was collected there.

4 Discussion

In the present study, the SEM topographies of the residual indent impressions from different groups of nanoindentation displayed distinct diversity, which is coherent with the data of mechanical properties obtained from nanoindentation tests. Here, two points deserve our attention. Firstly,

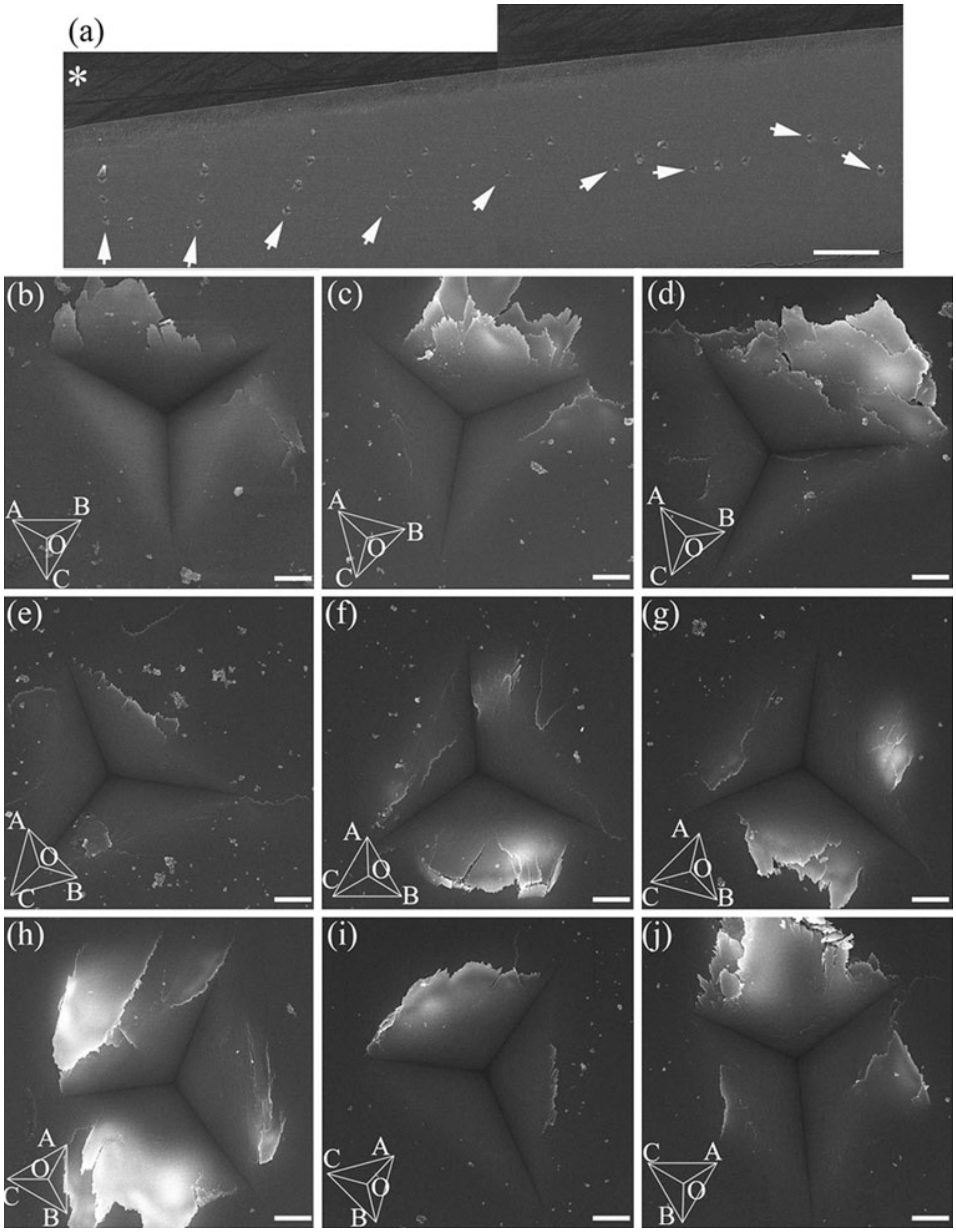

Fig. 3 SEM micrographs of the impressions. **a** The low-magnification image of the nine groups of nanoindentations indicated by *white arrowheads*. The *asterisk* indicates the resin for embedding. **b–j** the typical images of indent impressions with angles from 0° to 120°, with the sketch profiles labeled by OA, OB, and OC. The scale bar in **a** is 100 μm, and the others are 2 μm

the morphologies of indent impressions in longitudinal section of enamel were not typically equilateral triangle shapes, which implied that the anisotropy of enamel existed and that the cracks expanded differently along different directions. Secondly, the topographies reflected the distributions and accumulating directions of the pile-up around the impressions. In the Oliver–Pharr's method, the contact area and the pile-up accumulation at the three edges of the triangular impression should be accounted for hardness measurement [12]. In our study, the accumulations were found mainly along the orientation of enamel rods, which indicated that the cracks expanded much more easily along the rods than in the other directions. The anisotropy of cracks propagation resulted in the varied sizes of impressions and the alterations of the calculated values of hardness and elastic modulus.

Generally, there were three possible factors for the variations of mechanical properties. The first is the

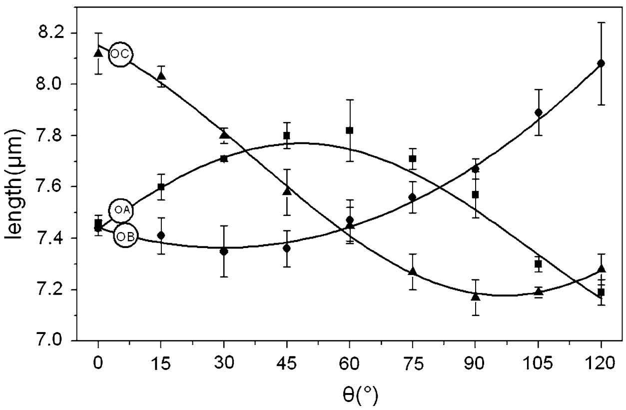

Fig. 4 The three edge lengths of indent impressions (OA, OB, and OC) are extended or shortened as the indenter rotates from 0° to 120°

nanoindentation position in the testing area, i.e., the distances between the nanoindentation impressions and the enamel surface. The second is the diversity among different enamel samples. The third was the inherent factor caused by the special structure of enamel. Analysis of the data was conducted with unbalanced general linear model (GLM), quadratic functions regression analysis, as well as two-way ANOVA for significance testing at the 95% confidence level. The statistical results were consistent with each other. The first two factors mentioned above were proved to have no appreciable effects on the mechanical anisotropy, while the angles of indenter rotation relative to enamel rods contributed to the diversity. Furthermore, no causal relationship was approved to exist between their mixed interactive effects. Therefore, we could conclude that the anisotropic mechanical properties were caused by the relative orientations of the indenter and the parallel-aligning enamel rods. In the testing area of the longitudinal section of outer enamel, the crystals lie parallel to the rod axis along the center and perpendicular to DEJ [13]. Occurrence of crack extensions were witnessed more frequently vertical to the crystals and rods than along them, and they expand much more easily in the latter direction [10]. It was conceivable that the elastic moduli in the two directions were differential, depending on their orientations to the crystals and rods.

Based on these results above, it could be concluded that enamel could not be modeled as a homogeneous and isotropic matrix phase. Therefore, a generalized self-consistent model has been established to identify the significant anisotropy as a function of the indenter relative to the rods' direction. For simplicity, only the 2-D components were considered, as shown in Fig. 5. As the cracks expanded differently vertical to or along the rods, the relative elastic moduli in two directions (Ex, Ey) were defined. And θ represented the angle between the indenter and the rods' direction. The relevant components of stress (F_x, F_y) and strains (S_x, S_y) in two directions were calculated by the following relations:

$$F_x = F \cdot \sin\theta \tag{1}$$

$$F_y = F \cdot \cos\theta \tag{2}$$

$$S_x = \frac{F_x}{E_x} = \frac{F\sin\theta}{E_x} \tag{3}$$

$$S_y = \frac{F_y}{E_y} = \frac{F\cos\theta}{E_y} \tag{4}$$

Then, the strains parallel to the stress "F" in different orientations were equal to the lengths of the three edges of nanoindentation impressions (L_{OA}, L_{OB}, and L_{OC}).

$$L_{OC} = L_x + L_y = S_x \cdot \sin\theta + S_y \cdot \sin\theta = \frac{F\sin^2\theta}{Ex} + \frac{F\cos^2\theta}{Ex} = k_1 + k_2\cos 2\theta \tag{5}$$

where, $k_1 = \frac{F(E_x+E_y)}{2E_xE_y}$, $k_2 = \frac{F(E_x-E_y)}{2E_xE_y}$, $\theta \in [0°, 120°]$

In this way, the other two strains could be deduced by analogy.

$$L_{OA} = k_1 + k_2\cos 2(\theta + 120°) \tag{6}$$

$$L_{OB} = k_1 + k_2\cos 2(\theta - 120°) \tag{7}$$

Based on these functions, the academic simulation of the relationships between OA, OB, OC and the angles were shown in Fig. 5c. Compared with the corresponding experimental data (Fig. 4), the model was closer to the truth and resembled with the experimental observations.

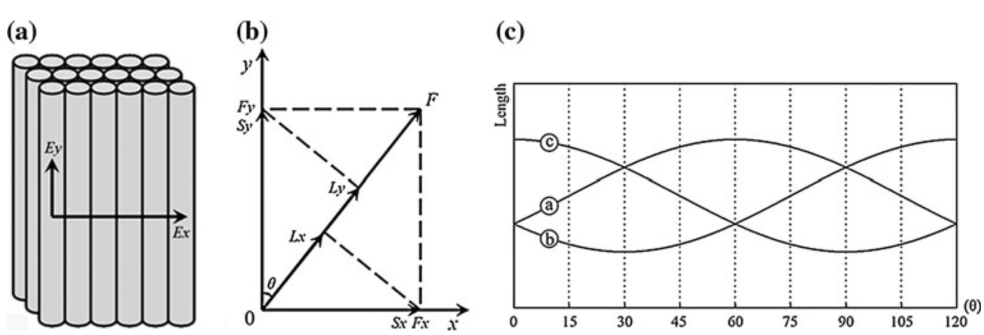

Fig. 5 **a** The decomposition of the elastic modulus "E" in testing area which consists of parallel-aligned enamel rods. **b** schematic drawing of the resolution of shearing force "F". **c** the academic simulation of the functions between OA, OB, OC and the relative angles (θ)

As a result, the bearing area (S) was approximately related to the angles,

$$S = \frac{\sqrt{3}}{4}(L_{OA} \cdot L_{OB} + L_{OA} \cdot L_{OC} + L_{OB} \cdot L_{OC}) = \frac{\sqrt{3}}{4}\left(3k_1^2 - k_2^2 + \frac{\sqrt{3}}{2}k_2^2 \cdot \sin 4\theta\right) \quad (8)$$

5 Conclusions

In this preliminary experiment, it was confirmed that the relative orientations of the indenter to the enamel rods' direction did effect on the elastic modulus, hardness and the shapes of the impressions. The main cause of the anisotropy was that the parallel arrangement of hydroxyapatite crystals and enamel rods triggered the micro-cracks expanding in preferred orientation. Therefore, unless the nanoindentations were carried out in the same orientation relative to the rods, the enamel should be modeled as an anisotropic material.

Acknowledgments This work was in part supported by National Basic Research Program of China, grant no 2005CB623905. Mature human molars and parts of the experimental service were provided by The China Crest Research Institute of P&G in Beijing.

References

1. Cui FZ, Ge J. New observations of the hierarchical structure of human enamel, from nanoscale to microscale. J Tissue Eng Regen M. 2007;1:185–95.
2. Balooch M, Wu-Magidi IC, Balazs A, Lundkvist AS, Marshall SJ, Marshall GW, et al. Viscolelastic properties of demineralized human dentin in water with atomic force microscopy (AFM)-based indentation. J Biomed Mater Res. 1998;40:539–44.
3. Marshall SJ, Balooch M, Habelitz S, Balooch G, Gallagher R, Marshall GW. The dentin–enamel junction—a natural, multilevel interface. J Eur Ceram Soc. 2003;23:2897–904.
4. Habelitz S, Marshall SJ, Marshall GW, Balooch M. Mechanical properties of human dental enamel on the nanometer scale. Arch Oral Biol. 2001;46:173–83.
5. Cuy JL, Mann AB, Livi KJ, Teaford MF, Weihs TP. Nanoindentation mapping of the mechanical properties of human molar enamel. Arch Oral Biol. 2002;47:281–91.
6. Finke M, Hughes JA, Parker DM, Jandt KD. Nanomechanical properties of in-situ demineralised human enamel measured by AFM nanoindentation. Surf Sci. 2001;491:456–67.
7. Marshall GW, Balooch M, Gallagher RR, Gansky SA, Marshall SJ. Mechanical properties of the dentinoenamel junction: AFM studies of nanohardness, elastic modulus and fracture. J Biomed Mater Res. 2001;54:87–95.
8. Nizam BRH, Lim CT, Chng HK, Yap AUJ. Nanoindentation study of human premolars subjected to bleaching agent. J Biomech. 2005;38:2204–11.
9. Xu HHK, Smith DT, Jahanmir S, Romberg E, Kelly JR, Thompson VP, et al. Indentation damage and mechanical properties of human enamel and dentin. J Dent Res. 1998;77:472–80.
10. Iwamoto N, Ruse ND. Fracture toughness of human dentin. J Biomed Mater Res. 2003;66A:507–12.
11. Oliver WC, Pharr GM. An improved technique for determining hardness and elastic modulus using load and displacement sensing indentation experiments. J Mater Res. 1992;7:1564–83.
12. Beegan D, Chowdhury S, Laugier MT. A nanoimdentation study of copper films on oxidized silicon substrates. Surf Coat Tech. 2003;176:124–30.
13. Ge J, Cui FZ, Wang XM, Feng HL. Property variations in the prism and the organic sheath within enamel by nanoindentation. Biomaterials. 2005;26:3333–9.